URA6 mutations provide an alternative mechanism for 5-FOA resistance in *Saccharomyces cerevisiae*

Joseph O. Armstrong[1+], Pengyao Jiang[1,2,+], Skyler Tsai[1], Megan My-Ngan Phan[1], Kelley Harris[1], Maitreya J. Dunham[1*]

[1]Department of Genome Sciences, University of Washington,
[2]Center for Mechanisms of Evolution, Biodesign Institute, School of Life Sciences, Arizona State University[2]

[+] Contributed equally
* Corresponding author

Abstract
URA3 is frequently used in the yeast community as the mutation target for 5-fluoroorotic acid (5-FOA) resistance. We identified a novel class of *ura6* mutants that can grow in the presence of 5-FOA. Unlike *ura3* mutants, *ura6* mutants remain prototrophic and grow in the absence of uracil. In addition to 5-FOA resistance, we found that mutations to *URA6* also confer resistance to 5-fluorocytosine (5-FC) and 5-fluorouracil (5-FU). In total, we identified 50 unique missense mutations across 32 residues of *URA6*. We found that 28 out of the 32 affected residues are located in regions conserved between *Saccharomyces cerevisiae* and three clinically relevant pathogenic fungi. These findings suggest that mutations to *URA6* present a second target for mutation screens utilizing 5-FOA as a selection marker as well as a potential mode of resistance to the antifungal therapeutic 5-FC.

Introduction

The *URA3* locus is a versatile tool for yeast geneticists and is used in a wide range of applications involving plasmid transformation, recombination, and mutation assays (Lang and Murray 2008; Kaneko et al. 2009; Boeke, LaCroute, and Fink 1984). A functional copy of *URA3* can be positively selected for by growing cells in the absence of uracil, or selected against, by growing cells in the presence of 5-FOA. 5-FOA is a fluorinated analog of orotic acid (OA), which is a metabolite in the *de novo* pyrimidine synthesis pathway upstream of Ura3. Both OA and 5-FOA are metabolized by the major and minor forms of orotate phosphoribosyltransferases encoded by *URA5* and *URA10* to form OMP and 5-fluoroorotidine monophosphate (5-FOMP), respectively. 5-FOMP is metabolized into 5-fluorouridine monophosphate (5-FUMP). The toxicity of 5-FOA is due to the subsequent conversion of 5-FUMP to 5-fluorodeoxyuridine monophosphate (5-FdUMP) and 5-fluorouridine triphosphate (5-FUTP) (Longley, Harkin, and Johnston 2003; Vermes, Guchelaar, and Dankert 2000). Cells with a loss of function mutation to *URA3* are resistant to 5-FOA because 5-FOMP can no longer be metabolized (Boeke, LaCroute, and Fink 1984). A loss of function mutation to *URA3* ablates the *de novo* pyrimidine synthesis pathway, and *ura3* mutants must salvage uracil from the environment to grow.

URA3 has been used as a mutation reporter in yeast genetics research for multiple decades (Lang and Murray 2008, 2011; Kiktev et al. 2018; Williams et al. 2021; Zhou et al. 2021; Lee et al. 1988). Although *URA3* is well known in the literature to be the primary target for 5-FOA resistance, there are unexplained instances where cells containing a wild-type copy of *URA3* were resistant to 5-FOA. For example, 10% of mutants that were discovered through a fluctuation assay (Lang and Murray 2008) contained a wild-type copy of *URA3*. More astonishingly, Boeke et al. reported that only 5-10% of a set of UV-induced 5-FOA mutants contained mutations to *URA3 (Boeke, LaCroute, and Fink 1984)*. The genetic cause of these 5-FOA-resistant cells containing a wild-type copy of *URA3* is unknown.

When we recently sought to use *URA3* as a mutation reporter, we unexpectedly found a large number of mutant colonies containing wild-type *URA3* that readily grew in the presence of 5-FOA. These mutants also grew readily in the absence of uracil, confirming that the pyrimidine *de novo* synthesis pathway was functional. Using whole genome sequencing, we confirmed that all resistant colonies with wild-type *URA3* had mutations to *URA6*, which has been previously linked to 5-FOA resistance, but not thoroughly characterized (Nivedita, Aitchison, and Baliga 2021; McAtee 2013). In addition to 5-FOA resistance, we also found that *ura6* mutants are resistant to fluorinated pyrimidine derivatives such as 5-fluorocytosine (5-FC) and 5-fluorouracil (5-FU), which are incorporated into the pyrimidine salvage pathway. To our knowledge, *URA6* is the sole mutable target capable of providing cross resistance to fluorinated prodrugs incorporated into both the pyrimidine synthesis and salvage pathways. Mutations to *URA6* represent a novel mechanism of cross-resistance to fluorinated pyrimidine analogs. We propose a working model in an attempt to describe the mechanism of resistance of *ura6* mutants with our current understanding of the *de novo* pyrimidine synthesis and salvage pathways.

Results

A novel class of ura6 mutants confers 5-FOA resistance in the absence of ura3 mutations

We discovered a new class of mutants that can grow in 5-FOA medium with the wildtype *URA3* allele in a haploid strain. A large number of cells (on the order of 10^8 for each sample) were plated to 5-FOA intended to identify *de novo* mutations to *URA3*. The initial inoculants were grown in synthetic complete media without uracil (SC-ura) media, which was to exclude all mutations that occurred in the *URA3* gene during the overnight growth. We used a pooled sequencing approach aiming to obtain the mutation spectrum of the *URA3* gene, similar to a previously published method using *CAN1* as a reporter gene (Jiang et al. 2021; Jiang, Ollodart, and Dunham 2022). To our surprise, we were able to call only 0-56% in *URA3* of the total number of mutants pooled in different samples (See Methods and Supplementary Figure 1 for details). We used Sanger sequencing to sequence the *URA3* locus from individual mutant clones contained within two pools and found that 19 out of 24 mutant clones tested did not show any mutations in *URA3.* This was surprising because all the mutants we isolated grew stably in the 5-FOA media. These mutants can grow stably in 5-FOA media without supplying uracil, whereas *ura3* mutants cannot (Fig. 1A). To our knowledge, no previously identified mutations permit growth in 5-FOA without uracil supplementation.

To uncover the genetic basis of the 5-FOA resistant and prototrophic mutants, we performed whole genome sequencing of ten individual clones. We found a missense mutation in the coding region of *URA6* in each of the clones we sequenced. These mutations occupy four different sites along the gene. Five mutants have the same mutation at the 31st amino acid, changing a G to a T, converting a Threonine to an Asparagine. These mutant clones are not identical since they also have unique mutations in other parts of the genome. However, multiple hits of the same site do not necessarily represent independent mutation events. To obtain a comprehensive distribution of mutations in *URA6* in our initial experiments, we used PCR to amplify the *URA6* locus from previously pooled mutants and performed Illumina sequencing and mutation calling. We recovered an additional 243 *ura6* mutants that gave rise to 5-FOA resistance (Supplementary Figure 2). We identified a total of 50 unique mutations in *URA6,* all of which are missense mutations (Supplementary Table 1). We isolated eight individual *ura6* mutants from these pools for further quantitative characterization. We tested a heterozygous knockout for *URA6* and found that they were no longer resistant to 5-FOA, which suggests that *ura6* mutations are recessive.

Mutations to URA6 provide cross resistance to 5-FU and 5-FC in addition to 5-FOA

While we initially discovered the *ura6* mutants from their resistance to 5-FOA, we hypothesized that the *ura6* mutants we identified would also be resistant to 5-FC and 5-FU since Ura6 lies at the junction of the pyrimidine synthesis and salvage pathways (Fig. 1B). Like 5-FOA, 5-FC and 5-FU are not inherently toxic to cells; however, in wild type cells, all three fluorinated pyrimidine derivatives can be converted into the cytotoxic compounds 5-FUTP and 5-FdUMP. These fluorinated pyrimidine derivatives share a common downstream metabolite in 5-FUMP, which is a substrate of Ura6, and a precursor to both 5-FUTP and 5-FdUMP. Previous studies found mutations to *URA6* conferred resistance to 5-FC in both pathogenic fungi and *S. cerevisiae* (Durand et al. 2023; Chang et al. 2021). We therefore explored whether the *ura6* mutants discovered in our study were resistant to the fluorinated prodrugs 5-FC and 5-FU in addition to 5-FOA using a growth rate assay.

To quantify the resistance of *ura6* mutants to the three fluorinated prodrugs, we measured growth in the following media: minimal media (MM), MM+5-FOA, MM+5-FU, MM+5-FC, synthetic complete media (SC), and SC-uracil (Fig. 1C, Supplementary Figure 3). Wild-type cells can undergo approximately one doubling in the presence of the fluorinated prodrugs. To account for the slight growth of the wild-type cells, we calculated the area under the growth curve (AUC) to compare the growth of the wild-type strain and the *ura6* mutants in the various media types (Fig. 1D). Wild-type cells grew more robustly than *ura6* strains in MM (Welch's two sample T test, p=0.006236). Wild-type cells only have residual growth in MM+FC, MM+FU, and MM+5-FOA, while *ura6* mutants have robust growth in 5-FC and 5-FU but impaired growth in 5-FOA (Fig. 1D).

The *ura6* mutants we identified grow equally well in MM and MM with 5-FC/FU (Fig. 1C), suggesting adding 5-FC and 5-FU has little impact on the growth of *ura6* mutants. This is in

contrast to a recent comprehensive study on *FCY1* mutants in the salvage pathway (Després et al. 2022), which showed a strong trade-off in growing in cytosine compared to media containing 5-FC — mutants that were highly resistant to 5-FC grew poorly in the presence of cytosine. We do not see a tradeoff between growth rates in the presence of any fluorinated drugs for *ura6* mutants, but rather a positive correlation between the two (Supplementary Figure 4).

ura6 mutants are not exclusively temperature sensitive

Previously identified *ura6* mutants (e.g. *ura6-1, ura6-4, ura6-5*) are temperature-sensitive (Liljelund and Lacroute 1986; Berg et al. 2020), showing permissive growth at 30°C and thermosensitivity at 37°C. To examine the isolated *ura6* mutants for temperature sensitivity, we quantified the growth rate for each mutant in MM and MM+5-FOA. Of the eight individual mutants we isolated for phenotyping, only one (I102N) was unable to grow in MM at 37°C (Fig. 1E). Notably, this I102N mutant also grew significantly worse than other mutants at 30°C in MM, MM+5FC, MM+5FU and MM+5-FOA (Fig. 1C, Supplementary Figure 5). Other than the I102N mutation, we do not observe a difference between the growth of the other isolated mutants at 30°C and 37°C, which distinguishes them from previously identified temperature-sensitive alleles (Fig. 1E).

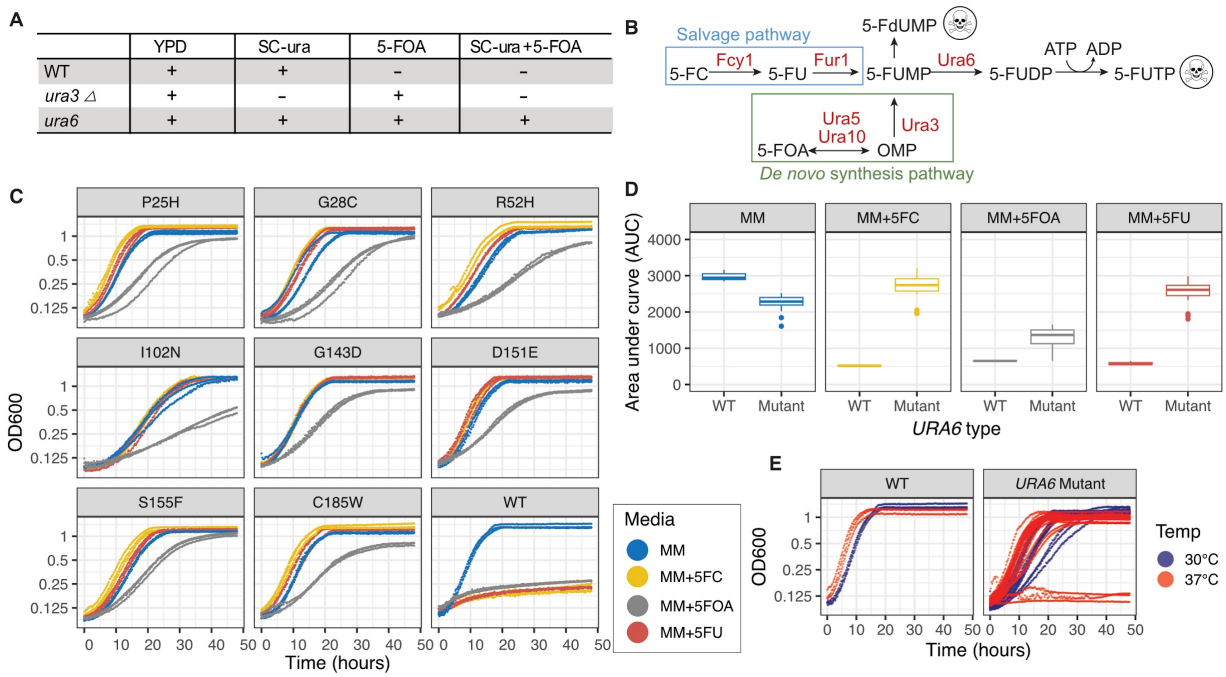

Figure 1. Growth of *ura6* mutants in media containing toxic fluorinated pyrimidine analogs. A) Summary comparison of qualitative growth phenotypes across WT, *ura3, and ura6* mutants in YPD, SC-ura, 5-FOA, SC-ura +5-FOA. "+" indicates growth, and "-" indicates lack of growth. B) *URA6* lies at the junction of the pyrimidine synthesis and salvage pathways. The fluorinated drugs 5-FC and 5-FU are incorporated into the pyrimidine salvage pathway. 5-FOA is incorporated into the pyrimidine synthesis pathway. The production of 5-FdUMP and 5-FUTP from the fluorinated prodrugs leads to toxicity. C) Growth curves for three biological replicates of *ura6* mutants and wild-type in MM, MM+5-FOA, MM+5FC, MM+5FU measured at 30°C. D) Area under the growth curve (AUC) measurements for growth for *ura6* mutants and wild-type strains grown in MM, MM+5-FOA, MM+5FC, MM+5FU measured at 30°C. E) Growth curves for three biological replicates of individual *ura6* mutants and wild type strains grown in MM at 30°C and 37°C.

Mutations to URA6 that cause cross resistance to 5-FC, 5-FU, and 5-FOA typically occur in conserved regions

In total, we identified 50 unique missense mutations across 32 residues of *URA6* (Fig. 2). We compared the position of the mutations to domains annotated on UniProt (UniProt Consortium 2023). We found mutations at one of three reported ATP binding sites, and four of the six reported ribonucleoside 5'-phosphate binding sites; however, many of the mutations we identified do not overlap with known functional domains. Notably, the distribution of these 50 mutations is not random along the gene (Chi-square test, $p < 0.05$, Supplementary Figure 6, robust to different bin sizes). The first ATP binding site and its adjacent sequences, close to amino acid position 25, appear to be especially enriched for mutations that confer resistance to 5-FOA.

We then compared the positions of *ura6* mutants in our study to the variation in *URA6* among 1,011 wild isolates of *S. cerevisiae* strains (Peter et al. 2018). All but one of the mutations we identified occur in residues that are conserved across all 1011 natural yeast isolates (Fig. 2, Supplementary Figure 7). We further compared the Ura6 amino acid sequence between *Saccharomyces cerevisiae* (S288C) and three clinically relevant pathogenic fungi, *Aspergillus fumigatus* (Af293), *Crytopcoccus neoformans* (JEC21), and *Candida albicans* (SC5314) using Ura6 protein sequences from FungiDB (Basenko et al. 2018). We found that *ura6* mutants are significantly enriched in residues that are conserved among all four species, with 28 of the 32 mutation sites in conserved residues (p = 1.866e-0.8, Fisher's exact test, Fig. 2). Taken together, these mutations are located in residues that are likely to be evolutionarily and functionally important.

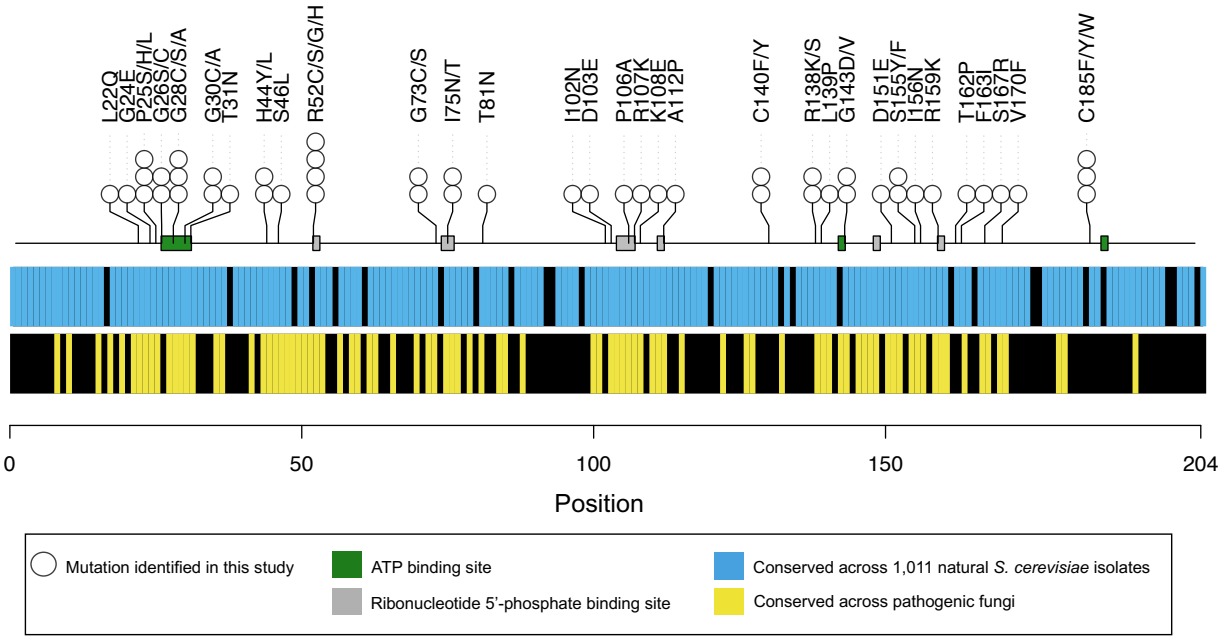

Figure 2. 5-FOA resistance mutations occur in evolutionarily conserved regions of *URA6*. White circles denote the missense Ura6 mutations identified in this study which confer resistance to fluorinated pyrimidine derivatives. Annotated binding sites are shown in green (ATP) and in gray (ribonucleotide 5'-phosphate). Conserved Ura6 residues between 1,011 natural *S. cerevisiae* isolates are shown in blue. Conserved residues between *S. cerevisiae* (S288C), *A. fumigatus* (Af293), *C. neoformans* (JEC21), and *C. albicans* (SC5314) are shown in yellow.

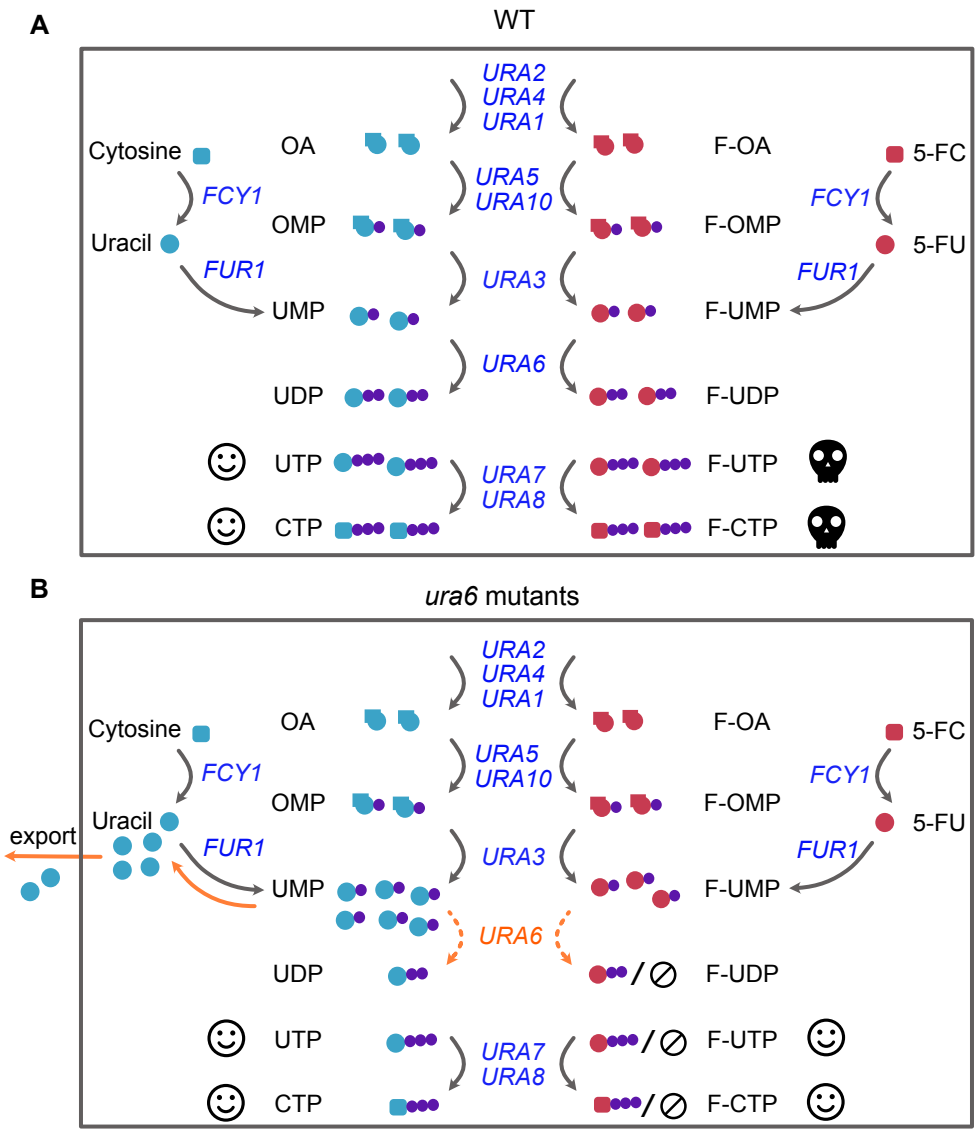

Figure 3. Working model for *ura6* mutants fluorinated prodrug resistance. A) The *de novo* pyrimidine synthesis and salvage pathway in the WT cells. The production of F-UTP and F-CTP leads to cell death. B) The *de novo* pyrimidine synthesis and salvage pathway in *ura6* mutant cells at 30°C. We propose that missense mutations can reduce Ura6 activity, leading to the build-up of UMP in the cells. A reduction in UMP kinase activity could enable these mutants to generate enough UTP and CTP for the cells to survive, but avoid producing enough F-UTP and F-CTP to lead to cell death.

Working model explaining the resistance of ura6 mutants to toxic fluorinated pyrimidine analogs

URA6 is an essential gene, which makes it unlikely that any of the 50 missense mutations we identified result in the complete loss of function of the enzyme. It is possible that some of these

mutations might cause the loss of Ura6's UMP kinase function, but only if the essentiality of *URA6* is due to the gene's function in some other pathway. In this case, an unknown compensatory pathway must also exist to convert UMP to UTP. Without further evidence of a compensatory pathway, we assume that our *ura6* mutants likely do have some UMP kinase activity and propose a model focused on how *ura6* mutants are resistant to fluorinated pyrimidines within our current understanding of the *de novo* pyrimidine synthesis and salvage pathways. We created a model that is compatible with our genetic and phenotypic data, which is summarized in Fig. 3.

In our working model, we propose that missense *ura6* mutations can reduce the flux of UMP to UDP (and correspondingly, F-UMP to F-UDP). This reduced activity leads to a build-up of both non-fluorinated and fluorinated UMP. Enough UMP is processed into UDP for the cell to grow, but not enough F-UMP is processed for the cell to die from the toxic downstream metabolites. This is supported by our growth assay where *ura6* mutants grow similarly in MM and MM+5-FC/FU (Fig. 2B, Rsq = 0.693). UMP accumulation has been previously observed in the *ts ura6-1* mutant (Liljelund and Lacroute 1986). Since the *ura6* mutants we identified are phenotypically comparable to *ura6-1* at 30°C, we can use biochemical assays from (Liljelund and Lacroute 1986) to infer how the function of *URA6* is impacted by an unspecified mutation. *ura6-1* mutants have a drastic (~1000-fold) decrease of uridylate kinase activity (dropped from 524 pmol/min/mg Ura6 in WT to 0.5 pmol/min/mg Ura6 for the *ura6-1* mutant) (Liljelund and Lacroute 1986), which leads to elevated UMP levels, consistent with a partial loss-of-function in *ura6.* Interestingly, despite the drastic decrease of Ura6 activity, only a 13-21% reduction of UTP and CTP levels was observed in *ura6-1* allele at 30°C, which allows the survival and growth of *ura6* mutants without supplying uracil. At 37°C, *ura6-1* mutants are no longer viable. This appears to be similar to the I102N mutant we characterized. The authors also observed that *ura6-1* cells excrete uracil upon the accumulation of UMP and suggested that the excretion of uracil may competitively inhibit the uptake of 5-FU. At 1mg/mL concentrations of 5-FU and 5-FC, the overwhelming amount of fluorinated drug available with respect to excreted uracil or cytosine implies that resistance to fluorinated prodrugs is not likely due to competitive inhibition of the membrane transporter, encoded by *FUR4*. We propose that either the build-up of UMP competitively inhibits the metabolism of 5-FUMP or that the reduced uridylate kinase activity favors UMP over 5-FUMP. Further studies are needed to elucidate the exact mechanism of fluorinated pyrimidine resistance of *ura6* mutants.

Discussion

The discovery of these *ura6* mutants may enable the design of more powerful mutation reporter assays. Our results imply that previously uncharacterized *URA3*+ mutants that contribute to 5-FOA resistance could be due to mutations in *URA6.* One reason that previous studies missed this could be due to the experimental design. Most 5-FOA-based selection for *URA3* is on higher frequency events, such as mitotic recombination, on the order of 10^{-5} events per genome per cell division(Jinks-Robertson and Petes 2021), which won't be affected by the low frequency of the *ura6* point mutants. Our study plated a large number of cells – on the order of 10^{8} for each

sample, including the overnight inoculant. We examined all *de novo* mutants that conferred resistance that arose during the incubation. On the contrary, standard fluctuation-based mutation assays dilute 10,000 fold from the overnight inoculant, making it less likely to observe any mutants that arose during the overnight incubation. Future studies should consider mutations to *URA6* when plating large quantities of cells to select for *URA3* using 5-FOA, especially when cells are pregrown in uracil dropout media. It is especially noteworthy that these *ura6* mutants cannot be easily selected against. In contrast, *CAN1* is the only major mutational target for the canavanine resistance phenotype, responsible for almost 100% of its mutants (Lang and Murray 2008; Jiang et al. 2021). For example, among 227 mutants that confer canavanine resistance, all of them have a mutation in the *CAN1* after individual Sanger sequencing (Lang and Murray 2008).

We were surprised to find that *ura6* mutants do not show an obvious growth trade-off in the presence or absence of fluorinated compounds, which was apparent in a recent study of mutations to *FCY1 (Després et al. 2022)*. The fact that *ura6* mutants can grow in MM, 5-FC, 5-FU, and 5-FOA, poses them in a unique category in comparison to WT or *ura3* cells, which can only grow in a subset of these conditions (Fig. 1A). Mutants like *ura6* can provide a possible stepping stone for adaptation — where a compromise is not a requirement when growing in a novel environment (Wang et al. 2024). It is also possible that we haven't explored all plausible environments in which *ura6* can show the trade-off. Quantitatively, we also observed that WT cells grow slightly better in MM in comparison to *ura6*, which means *ura6* cells will be outcompeted against in non-fluorinated conditions. Interestingly, the *ura6* mutants we identified tend to reside in conserved regions in pathogenic yeasts across large evolutionary distances. This suggests that evolution hasn't exploited the potential for *ura6* mutations to confer resistance to toxins that exist in nature. That being said, although most of the mutations we found occur in sites that are conserved across *S. cerevisiae* and pathogenic fungi, four mutation sites which confer resistance in *S. cerevisiae* are located in non-conserved regions. Since *ura6* mutations in *S. cerevisiae* can confer resistance to the common antifungal 5-FC, these sites may confer antifungal resistance in pathogenic yeast. However, given that there are many other genetic changes in pathogenic yeast in *URA6*, future studies are needed to elucidate the function and evolution of *URA6* in pathogenic yeast.

Acknowledgment

PJ was supported by a Burroughs Wellcome Fund Career Award at the Scientific Interface awarded to KH. J.O.A. acknowledges support from University of Washington Biological Mechanisms of Healthy Aging training grant. KH acknowledges additional support from a Searle Scholarship, a Sloan Research Fellowship, a Pew Biomedical Scholarship, and National Institute of General Medical Sciences Grant 1R35GM133428-01. The content is solely the responsibility of the authors and does not necessarily represent the official views of the Burroughs Wellcome Fund, the Kinship Foundation, the Sloan Foundation, the Pew Charitable Trust, HHMI, the NIH, or NIGMS.

Materials and Methods

Strains:

FY4 *MATα flo1::KanMx*, *flo9::NatMx*

Media:
Minimal media (MM): Yeast nitrogen base, without amino acids and without ammonium sulfate (1.7g/L), Ammonium Sulfate (5g/L), Dextrose (20g/L)

Minimal media + fluorinated prodrug (MM+5-FC, MM+5-FU, MM+5-FOA): A concentration of 1mg/mL was used for all fluorinated prodrug media.

Synthetic complete media (SC): Yeast nitrogen base, without amino acid and without ammonium sulfate (1.7g/L), Ammonium Sulfate (5g/L), Dextrose (20g/L), Adenine (0.019g/L), Arginine (0.019g/L), Aspartic Acid (0.096g/L), Glutamic Acid (0.096g/L), Histidine (0.019g/L), Isoleucine (0.077g/L), Leucine (0.077g/L), Lysine (0.058g/L), Methionine (0.019g/L), Phenylalanine (0.048g/L), Serine (0.384g/L), Threonine (0.192g/L), Tryptophan (0.077g/L), Tyrosine (0.058g/L), Uracil (0.019g/L), Valine (0.144g/L)

Synthetic complete media without uracil (SC-ura): Yeast nitrogen base, without amino acid and without ammonium sulfate (1.7g/L), Ammonium Sulfate (5g/L), Dextrose (20g/L), Adenine (0.019g/L), Arginine (0.019g/L), Aspartic Acid (0.096g/L), Glutamic Acid (0.096g/L), Histidine (0.019g/L), Isoleucine (0.077g/L), Leucine (0.077g/L), Lysine (0.058g/L), Methionine (0.019g/L), Phenylalanine (0.048g/L), Serine (0.384g/L), Threonine (0.192g/L), Tryptophan (0.077g/L), Tyrosine (0.058g/L), Valine (0.144g/L)

ura6 *mutant discovery and sequencing analysis*

The original experiment was set up to use *URA3* to quantify mutation rates across the lifespan of yeast. Overnight inoculants were grown in SC-ura media, which were subsequently labeled with magnetic beads. Continuous cultures with magnetics are set up to capture the mother cells, under three conditions, SC-ura without glucose, SC, and SC-ura. Mother and daughter cells from different time points (day 0, day 1, day 4, day 6) were harvested and tested for their mutation rates using 5-FOA resistance selection.

Generating the mutant pools follows the procedure in (Jiang et al. 2021; Jiang, Ollodart, and Dunham 2022), pooling roughly 35 mutants per pool. We used PCR to amplify the *URA3* locus and prepared the PCR product for Illumina sequencing using the Nextera XT kit. We used the same mutation calling pipeline as (Jiang et al. 2021), without excluding multi-nucleotide mutations. To identify mutations to *URA6*, we used PCR to amplify the *URA6* locus and prepared the PCR product for Illumina sequencing from the same pooled genomic DNA. The same mutation calling pipeline as *URA3* was used.

10 individual mutants were subjected to whole-genome sequencing using the Illumina DNA Flex Library Prep Kit and sequenced on Nextseq 550. We performed the variant calling pipeline as previously described (Taylor et al. 2022).

Quantification of cell growth

To quantify the growth of *ura6* mutants, three individual clones were isolated from eight unique mutants grown in 200μL minimal media in 96-well plates for 24 hours at 30°C. The 24-hour cultures were resuspended and 2μL of each culture was transferred into 200 μL of the following media types: synthetic complete media (SC media), synthetic media minus uracil (SC-ura), minimal media (MM), minimal media with 5-FOA (MM+5-FOA, 1mg/mL), minimal media with 5-FU (MM+5FU, 1mg/mL), and minimal media with 5-FC (MM+5FC, 1mg/mL). A Biotek Synergy

H1 plate reader was used to monitor optical density every 15 minutes over the course of 48 hours. Growth measurements were conducted at both 30°C and 37°C to assess temperature sensitivity. To quantify the area under the growth curves (AUC) we used the "gcplyr" R package (Blazanin 2024).

Conservation

To identify the natural variation of Ura6 within *Saccharomyces cerevisiae* strains, amino acid sequences of Ura6 from the 1,011 *S. cerevisiae* natural isolate collection were used to perform a within-species alignment. We used MAFFT v 7.487 (Katoh and Standley 2013) to perform multiple sequence alignments with an accurate alignment option (mafft-linsi) with default parameters.

To identify conserved regions between pathogenic fungi and *Saccharomyces cerevisiae* we compared the amino acid sequence of Ura6 in *S. cerevisiae* (S288C), *A. fumigatus* (Af293), *C. neoformans* (JEC21), and *C. albicans* (SC5314) using Clustal alignments collected from from FungiDB. We only scored residues that were conserved between all four species. We used the bioconductor package, LollipopPlot (Ou and Zhu 2019) to visualize the positions of the mutations and their relative frequency and a custom R script to generate the conservation tracks.

References

Basenko, Evelina Y., Jane A. Pulman, Achchuthan Shanmugasundram, Omar S. Harb, Kathryn Crouch, David Starns, Susanne Warrenfeltz, et al. 2018. "FungiDB: An Integrated Bioinformatic Resource for Fungi and Oomycetes." *Journal of Fungi (Basel, Switzerland)* 4 (1). https://doi.org/10.3390/jof4010039.

Berg, Matthew D., Yanrui Zhu, Joshua Isaacson, Julie Genereaux, Raphaël Loll-Krippleber, Grant W. Brown, and Christopher J. Brandl. 2020. "Chemical-Genetic Interactions with the Proline Analog L-Azetidine-2-Carboxylic Acid in *Saccharomyces Cerevisiae*." *G3* 10 (12): 4335–45.

Blazanin, Michael. 2024. "Gcplyr: An R Package for Microbial Growth Curve Data Analysis." *bioRxiv*. https://doi.org/10.1101/2023.04.30.538883.

Boeke, J. D., F. LaCroute, and G. R. Fink. 1984. "A Positive Selection for Mutants Lacking Orotidine-5'-Phosphate Decarboxylase Activity in Yeast: 5-Fluoro-Orotic Acid Resistance." *Molecular & General Genetics: MGG* 197 (2): 345–46.

Chang, Yun C., Ami Khanal Lamichhane, Hongyi Cai, Peter J. Walter, John E. Bennett, and Kyung J. Kwon-Chung. 2021. "Moderate Levels of 5-Fluorocytosine Cause the Emergence of High Frequency Resistance in Cryptococci." *Nature Communications* 12 (1): 3418.

Després, Philippe C., Angel F. Cisneros, Emilie M. M. Alexander, Ria Sonigara, Cynthia Gagné-Thivierge, Alexandre K. Dubé, and Christian R. Landry. 2022. "Asymmetrical Dose Responses Shape the Evolutionary Trade-off between Antifungal Resistance and Nutrient Use." *Nature Ecology & Evolution* 6 (10): 1501–15.

Durand, Romain, Jordan Jalbert-Ross, Anna Fijarczyk, Alexandre K. Dubé, and Christian R. Landry. 2023. "Cross-Feeding Affects the Target of Resistance Evolution to an Antifungal Drug." *PLoS Genetics* 19 (10): e1011002.

Hofmann, Heike. n.d. *Gglogo: R Package for Creating Sequence Logo Plots*. Github. Accessed March 28, 2024. https://github.com/heike/gglogo.

Jiang, Pengyao, Anja R. Ollodart, and Maitreya J. Dunham. 2022. “A Modified Fluctuation Assay with a *CAN1* Reporter in Yeast.” *Bio-Protocol* 12 (11): e4435.
Jiang, Pengyao, Anja R. Ollodart, Vidha Sudhesh, Alan J. Herr, Maitreya J. Dunham, and Kelley Harris. 2021. “A Modified Fluctuation Assay Reveals a Natural Mutator Phenotype That Drives Mutation Spectrum Variation within *Saccharomyces Cerevisiae*.” *eLife* 10 (September). https://doi.org/10.7554/eLife.68285.
Jinks-Robertson, Sue, and Thomas D. Petes. 2021. “Mitotic Recombination in Yeast: What We Know and What We Don’t Know.” *Current Opinion in Genetics & Development* 71 (December): 78–85.
Kaneko, Shohei, Tsutomu Tanaka, Hideo Noda, Hideki Fukuda, Rinji Akada, and Akihiko Kondo. 2009. “Marker-Disruptive Gene Integration and *URA3* Recycling for Multiple Gene Manipulation in *Saccharomyces Cerevisiae*.” *Applied Microbiology and Biotechnology* 83 (4): 783–89.
Katoh, Kazutaka, and Daron M. Standley. 2013. “MAFFT Multiple Sequence Alignment Software Version 7: Improvements in Performance and Usability.” *Molecular Biology and Evolution* 30 (4): 772–80.
Kiktev, Denis A., Ziwei Sheng, Kirill S. Lobachev, and Thomas D. Petes. 2018. “GC Content Elevates Mutation and Recombination Rates in the Yeast *Saccharomyces Cerevisiae*.” *Proceedings of the National Academy of Sciences of the United States of America* 115 (30): E7109–18.
Lang, Gregory I., and Andrew W. Murray. 2008. “Estimating the Per-Base-Pair Mutation Rate in the Yeast *Saccharomyces Cerevisiae*.” *Genetics* 178 (1): 67–82.
———. 2011. “Mutation Rates across Budding Yeast Chromosome VI Are Correlated with Replication Timing.” *Genome Biology and Evolution* 3 (June): 799–811.
Lee, G. S., E. A. Savage, R. G. Ritzel, and R. C. von Borstel. 1988. “The Base-Alteration Spectrum of Spontaneous and Ultraviolet Radiation-Induced Forward Mutations in the URA3 Locus of *Saccharomyces Cerevisiae*.” *Molecular & General Genetics: MGG* 214 (3): 396–404.
Liljelund, P., and F. Lacroute. 1986. “Genetic Characterization and Isolation of the *Saccharomyces Cerevisiae* Gene Coding for Uridine Monophosphokinase.” *Molecular & General Genetics: MGG* 205 (1): 74–81.
Longley, Daniel B., D. Paul Harkin, and Patrick G. Johnston. 2003. “5-Fluorouracil: Mechanisms of Action and Clinical Strategies.” *Nature Reviews. Cancer* 3 (5): 330–38.
McAtee, Christopher. 2013. “Non-Random Mutations in Yeast: An Examination of Yeast Genetics during Selection Cycling.” Edited by Eric J. Sorscher. The University of Alabama at Birmingham. http://login.ezproxy1.lib.asu.edu/login?url=https://www.proquest.com/dissertations-theses/non-random-mutations-yeast-examination-genetics/docview/1433367788/se-2.
Nivedita, Nivedita, John D. Aitchison, and Nitin S. Baliga. 2021. “Autophagy as a Mechanism for Adaptive Prediction-Mediated Emergence of Drug Resistance.” *Frontiers in Microbiology* 12 (September): 712631.
Ou, Jianhong, and Lihua Julie Zhu. 2019. “trackViewer: A Bioconductor Package for Interactive and Integrative Visualization of Multi-Omics Data.” *Nature Methods* 16 (6): 453–54.
Peter, Jackson, Matteo De Chiara, Anne Friedrich, Jia-Xing Yue, David Pflieger, Anders Bergström, Anastasie Sigwalt, et al. 2018. “Genome Evolution across 1,011 *Saccharomyces Cerevisiae* Isolates.” *Nature* 556 (7701): 339–44.
Taylor, Matthew Bryce, Ryan Skophammer, Alexa R. Warwick, Renee C. Geck, Josephine M. Boyer, yEvo Students, Margaux Walson, et al. 2022. “yEvo: Experimental Evolution in High School Classrooms Selects for Novel Mutations That Impact Clotrimazole Resistance in *Saccharomyces Cerevisiae*.” *G3* 12 (11). https://doi.org/10.1093/g3journal/jkac246.
UniProt Consortium. 2023. “UniProt: The Universal Protein Knowledgebase in 2023.” *Nucleic*

Acids Research 51 (D1): D523–31.
Vermes, A., H. J. Guchelaar, and J. Dankert. 2000. “Flucytosine: A Review of Its Pharmacology, Clinical Indications, Pharmacokinetics, Toxicity and Drug Interactions.” *The Journal of Antimicrobial Chemotherapy* 46 (2): 171–79.
Wang, Xuechun May, Julia Muller, Mya McDowell, and David A. Rasmussen. 2024. “Quantifying the Strength of Viral Fitness Tradeoffs between Hosts: A Meta-Analysis of Pleiotropic Fitness Effects.” *bioRxiv*. https://doi.org/10.1101/2023.12.16.571995.
Williams, Jessica S., Percy P. Tumbale, Mercedes E. Arana, Julian A. Rana, R. Scott Williams, and Thomas A. Kunkel. 2021. “High-Fidelity DNA Ligation Enforces Accurate Okazaki Fragment Maturation during DNA Replication.” *Nature Communications* 12 (1): 482.
Zhou, Zhi-Xiong, Scott A. Lujan, Adam B. Burkholder, Jordan St Charles, Joseph Dahl, Corinne E. Farrell, Jessica S. Williams, and Thomas A. Kunkel. 2021. “How Asymmetric DNA Replication Achieves Symmetrical Fidelity.” *Nature Structural & Molecular Biology* 28 (12): 1020–28.

Supplementary Figures

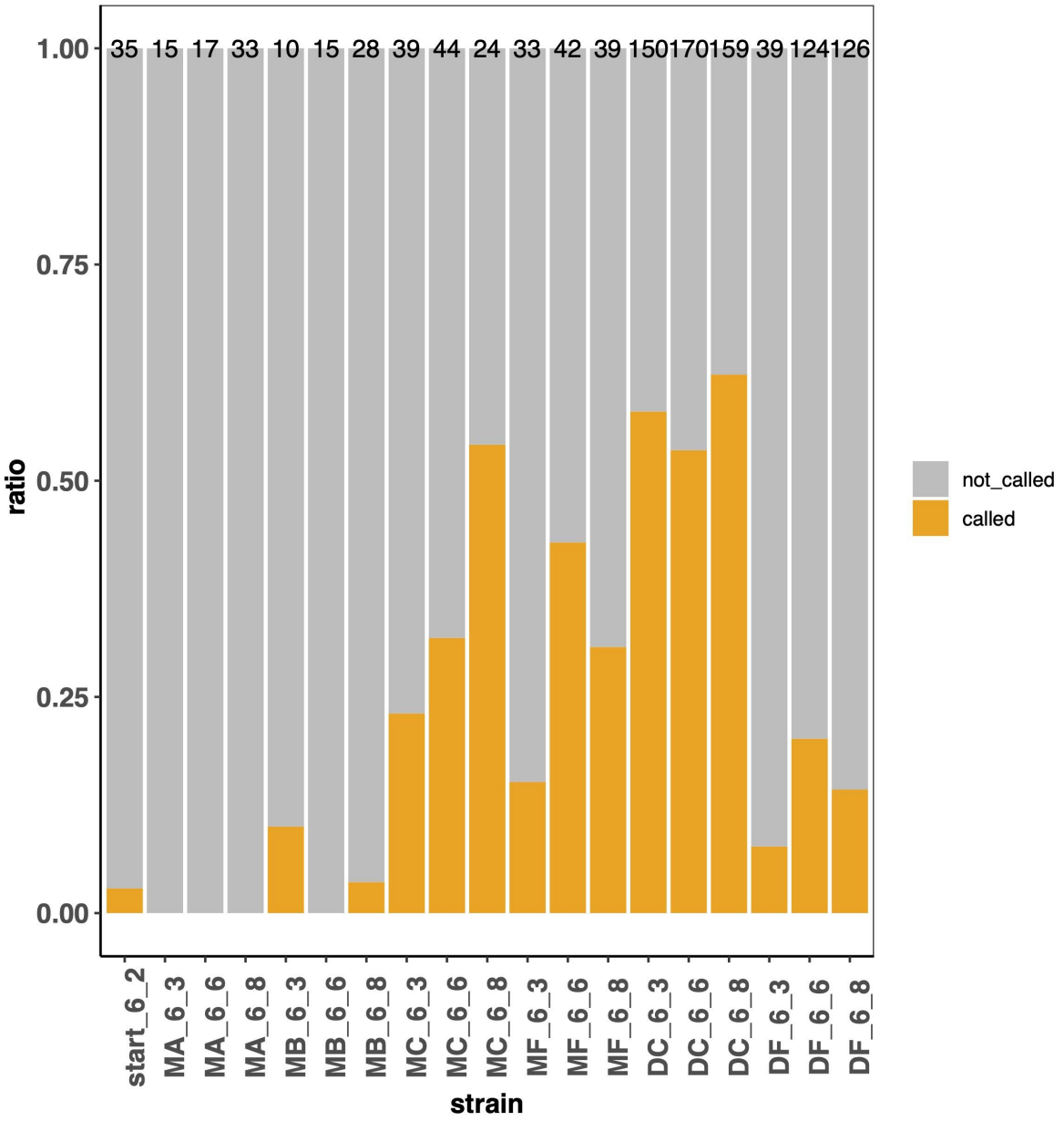

Supplementary Figure 1. The ratio of *ura3* mutants in each mutant sample. The number on the top of each bar shows the total number of individual mutants pooled in each sample. The orange bar shows the ratio of called *ura3* mutants from the computational pipeline after sequencing by the total number of mutants pooled. The large two numbers denote the date of the sample, for example, “6_2” means June 2. “Start” sample is the overnight inoculant. Samples begin with “M” are mother cells, “D” are daughter cells. The second letter denotes different growth conditions, “A” and “B” are SC-ura without no glucose, “C” and “D” are SC, “E”

and “F” are SC-ura.

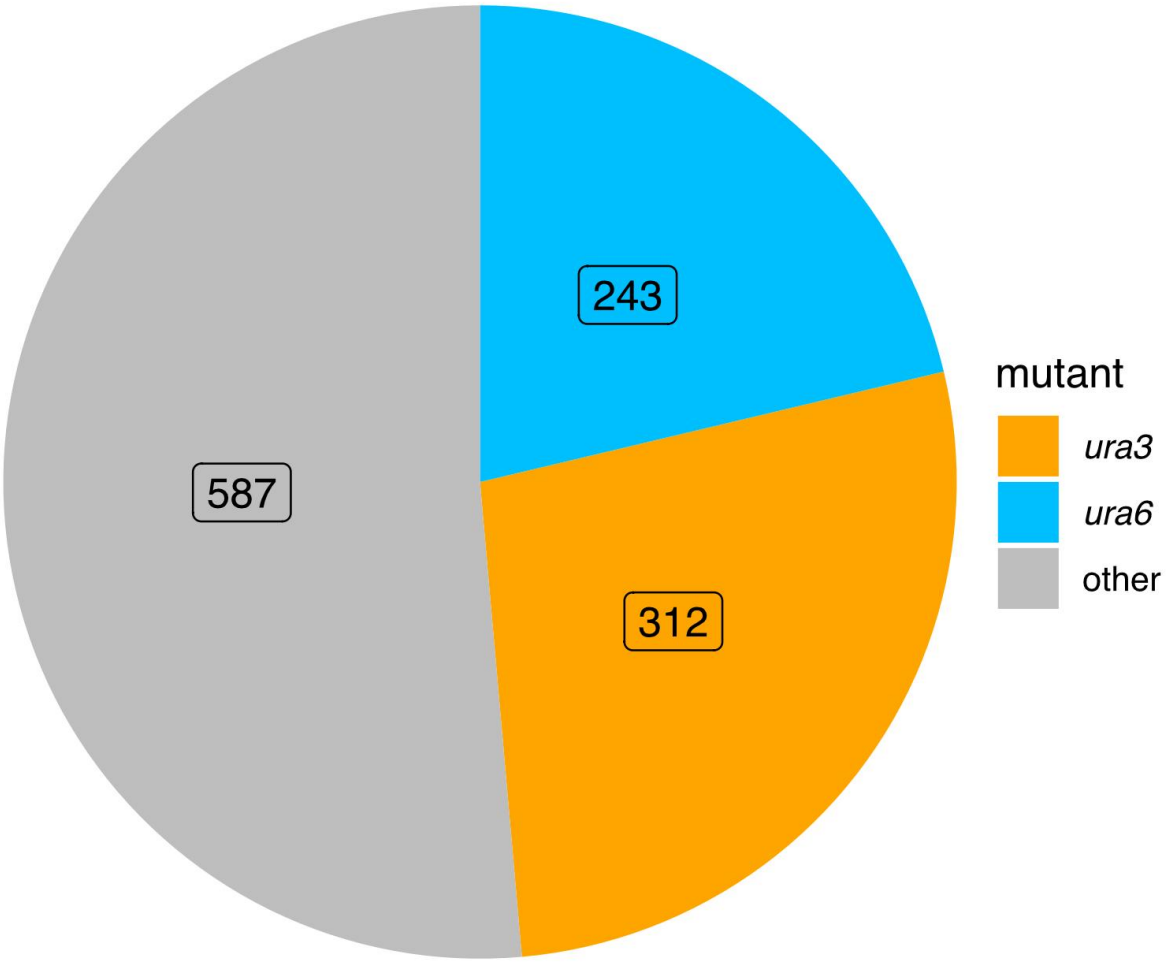

Supplementary Figure 2. A pie chart displaying *ura3 and ura6* mutants called across all mutant samples. Blue indicates the *ura6* mutants, and yellow indicates *ura3.* Grey indicates the remaining mutants that are pooled but not called either *ura3* or *ura6* in our pipeline.

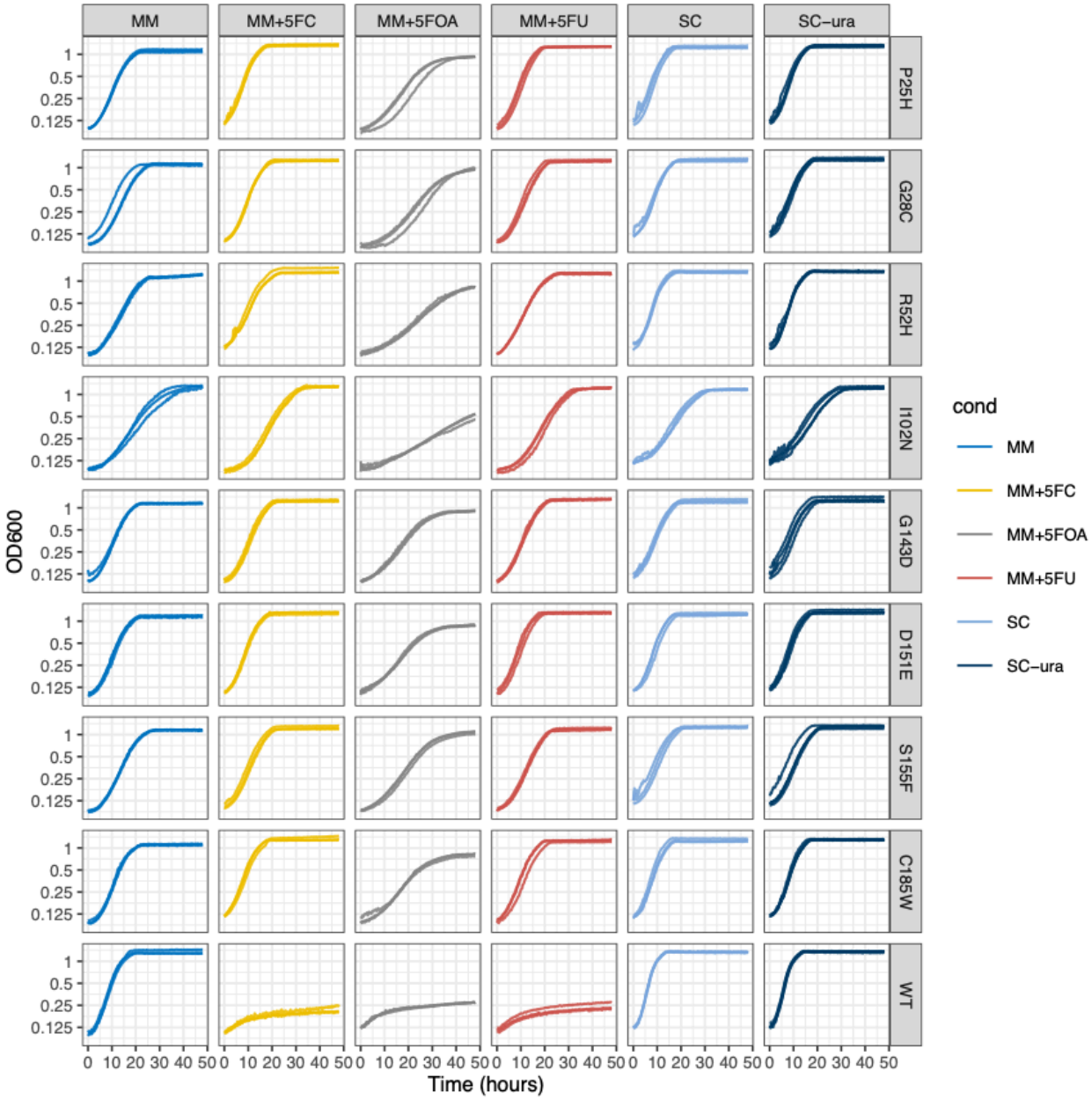

Supplementary Figure 3. Growth curves of wild type and *ura6* cultures grown in MM, MM+5FC, MM+5-FOA, MM+5FU, SC, and SC-ura media at 30°C

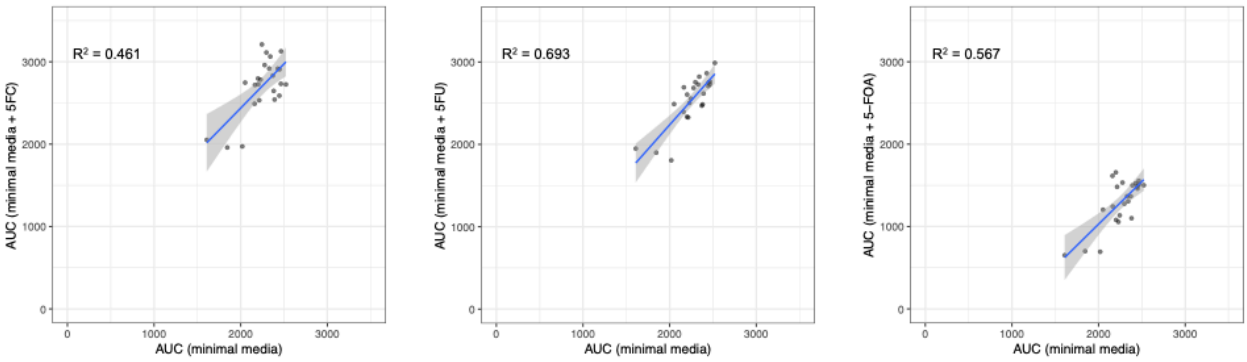

Supplementary Figure 4. Linear correlations of AUC measurements between MM and fluorinated drug containing media for *ura6* mutants.

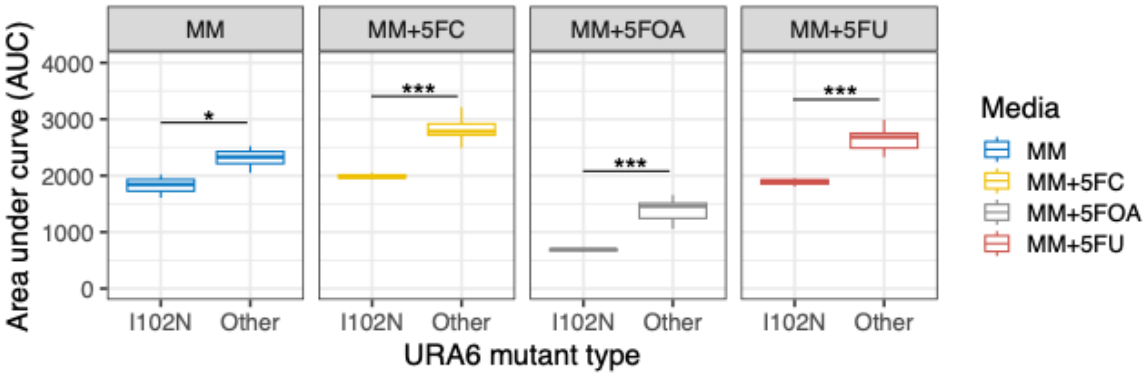

Supplementary Figure 5 : The temperature sensitive I102N mutant grows less robustly than the other isolated mutants in all media types. The difference in AUC between the I102N mutant and the rest of the *ura6* mutants was determined to be statistically significant across all media types (Welch's two sample T test, MM (p-value = 0.04728), MM+5FC (p-value = 2.264e-10), MM+5-FOA (p-value = 7.764e-06), MM+5FU (p-value = 1.428e-13))

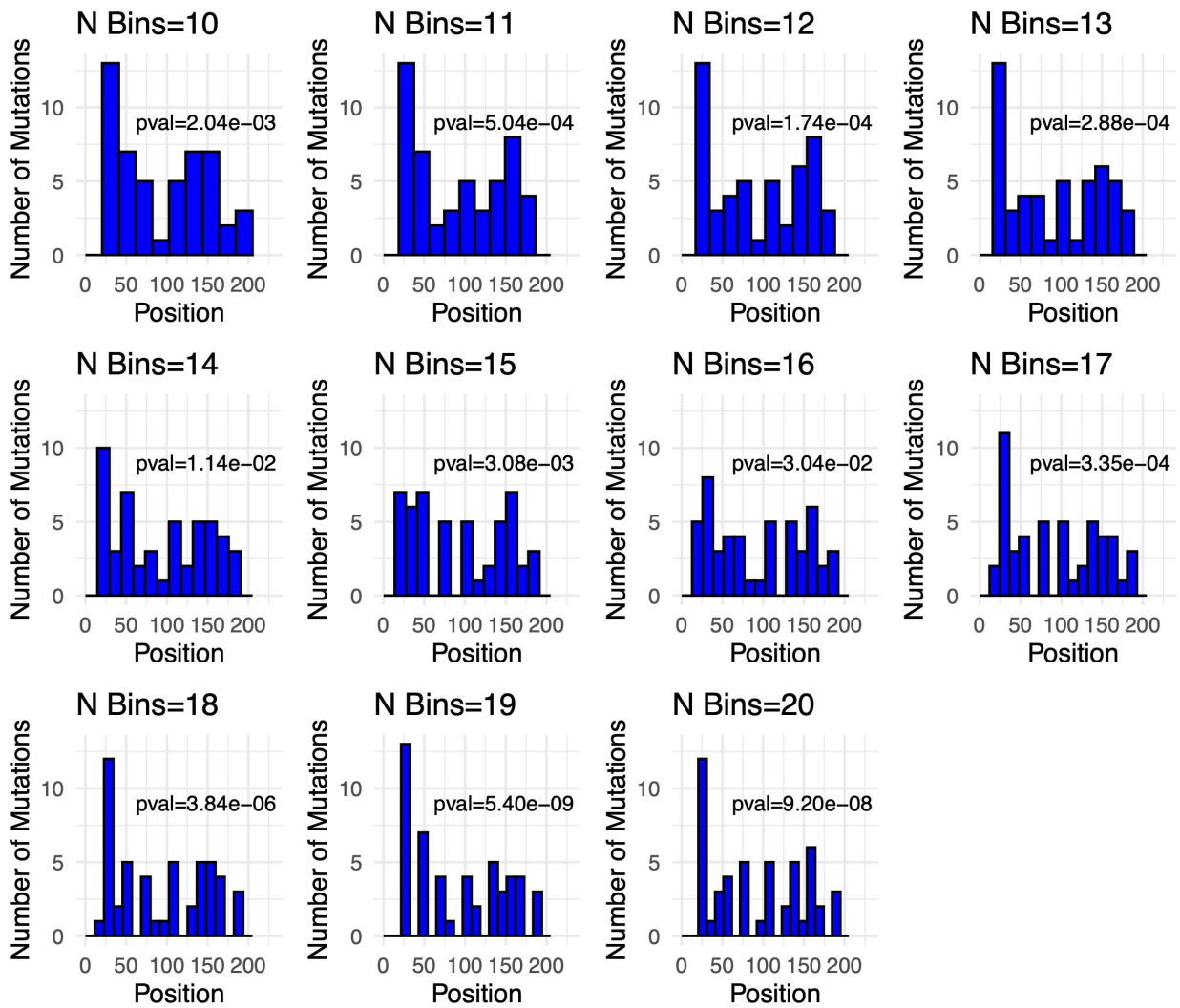

Supplementary Figure 6. Testing the uniformity of *ura6* distribution along the gene. Different bin sizes are tested. Ura6 sequence is divided into different bins. Each plot shows the number of unique mutants that are present in each bin, given the bin size. The chi-square tests are performed on the observed number of mutants per bin against the expected number of mutants if they are uniformly distributed. The *p-value* is shown for each bin size. An enrichment near position 25 is observed in most of the cases.

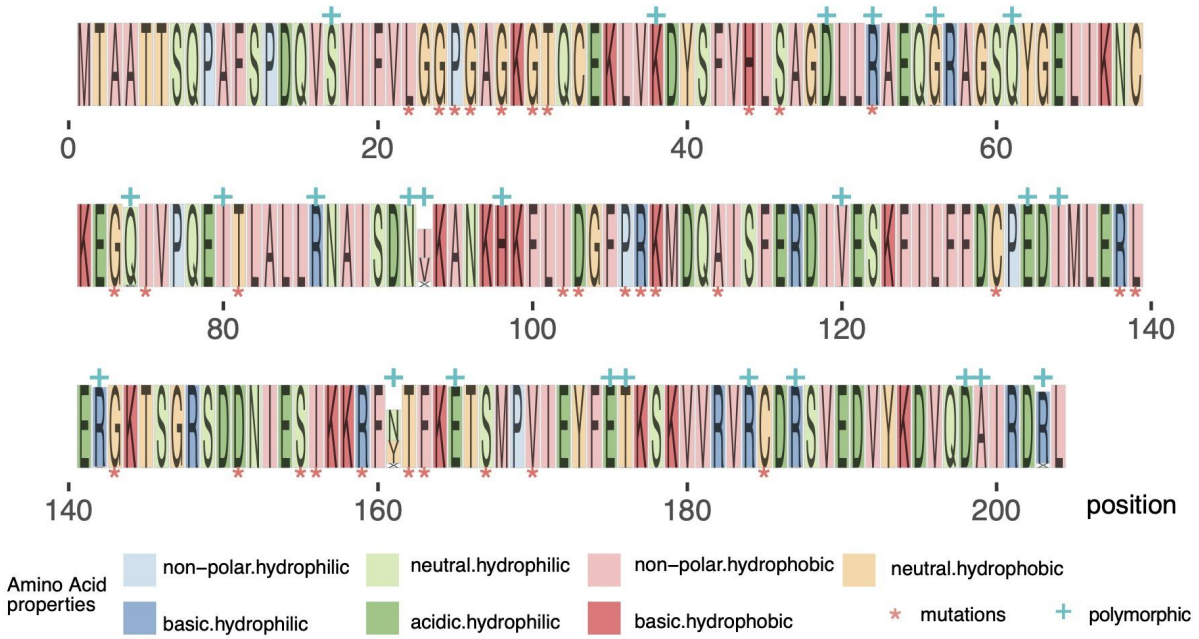

Supplementary Figure 7. The positions of unique missense mutations to *URA6* identified in this study compared with polymorphic sites in the 1011 *S. cerevisiae* collection. Logo plot (gglogo package(Hofmann, n.d.)) for the entire Ura6 based on all the polymorphisms in the 1011 *S. cerevisiae.* Sites that are polymorphic in the 1011 *S. cerevisiae* are marked with blue crosses. Unique *ura6* sites are marked with red asterisks.